Reconstruction of 2D Al$_3$Ti on TiB$_2$ in an aluminium melt

Reconstruction of 2D Al_3Ti on TiB_2 in an aluminium melt

T Qin and Z Fan

The EPSRC Centre-LiME, BCAST, Brunel University, Uxbridge, Middlesex UB8 3PH, UK

E-mail: `Ting.Qin@brunel.ac.uk`

Abstract. It has been widely considered that Al_3Ti is involved in the aluminium nucleation on TiB_2, although the mechanism has not been fully understood. In this paper molecular dynamics has been conducted to investigate this phenomenon at an atomistic scale. It was found that a two-dimensional Al_3Ti layer may remain on TiB_2 above the aluminium liquidus. In addition, the results showed that this 2D Al_3Ti undergoes interface reconstruction by forming a triangular pattern. This triangular pattern consists of different alternative stacking sequences. The transition region between the triangles forms an area of strain concentration. By means of this mechanism, this interfacial Al_3Ti layer stabilizes itself by localizing the large misfit strain between TiB_2 and Al_3Ti. This reconstruction is similar to the hdp-fcc interface reconstruction in other systems which has been observed experimentally [1].

1. Introduction

A common industrial practice to refine aluminium is to use Al-5Ti-B master alloy during the solidification process [2]. It has been demonstrated that TiB_2 alone does not refine α-Al [3]. Consequently, a small amount of excess titanium is required for grain refinement in aluminium, but the mechanism of how titanium acts is still strongly disputed [4, 5, 6, 7]. Because of the low misfit between Al_3Ti and Al, Al_3Ti has been shown to be a more potent nucleant than TiB_2 either by experiment or from simulations [8]. However, bulk Al_3Ti is thermodynamically unstable in molten aluminium with a titanium concentration of less than 0.15 wt.%. Experiment carried out by Schumacher and Greer showed that a layer forms between TiB_2 and aluminium [9], and they suggested that this layer could be Al_3Ti. However, how and why this layer of Al_3Ti can remain on TiB_2 requires further investigation.

The initial solidification stage known as nucleation intrinsically takes place at an atomistic level. Therefore, atomistic simulations can facilitate the understanding of this problem by using density functional theory (DFT) [10, 11] and molecular dynamics (MD) [12]. DFT calculations have suggested that a Al_3Ti-like thin layer could be thermodynamically stable on the top of TiB_2 prior to aluminium solidification [13]. On the other hand, the *ab initio* molecular dynamics simulations have not shown that a layer of Al_3Ti forms on the top of TiB_2 [14], which may be due to the time limitation of *ab initio* molecular dynamics.

It is well-known that Al_3Ti is very coherent with aluminium, and consequently this provides strong evidence that the excess amount of titanium could form a thin-layer Al_3Ti on the top of the TiB_2 surface. However, the misfit between Al_3Ti and TiB_2 is large. Despite their large misfit, how does this thin layer of Al_3Ti stay on TiB_2? This has been investigated by means of molecular dynamics in this paper.

2. Simulation procedure

MD simulations were carried out using the LAMMPS [15] and DL_POLY programs [16]. MD integrates Newton's equation of motion using the velocity-Verlet integration algorithm [17]. Therefore, a reliable interatomic potential is required for the Newton's equation . In this paper, the widely-used Al-Ti Finnis-Sinclair-type potential [18] parametrized by Zope and Mishin [19] was used. The lattice constants of TiB_2, Al_3Ti and aluminium are summarized in table 1. The

Table 1. Experimental lattice spacing of TiB_2, Al_3Ti and Al.

	structure	a (Å)	c (Å)	d (Å)	$\gamma(K^{-1})$	d_m (Å)
TiB_2[20]	hexagonal	3.030	3.229	3.030	3.56×10^{-6} [21]	3.0372
Al_3Ti[22]	tetragonal	3.8537	8.5839	2.8046	15.0×10^{-6} [23]	2.9116
Al [24]	fcc	4.05		2.864	27.9×10^{-6}[21]	2.9141

Here d and d_m are the atomic spacing at room temperature and the aluminium melting temperature, respectively. γ is the thermal expansion

orientational relationship between these three components has been suggested by experiments as [9]:

$$(0001)_{TiB_2}[11\bar{2}0]_{TiB_2}||(112)_{Al_3Ti}[20\bar{1}]_{Al_3Ti} \qquad (1)$$

and

$$(112)_{Al_3Ti}[20\bar{1}]_{Al_3Ti}||(111)_{Al}[11\bar{2}]_{Al}. \qquad (2)$$

Following the above relationship, misfit can be used to characterize their interface disregistry:

$$f = \frac{d - d_s}{d}, \qquad (3)$$

where d and d_s are the atomic spacing of the solidified crystal and its substrate. As a result, the misfit between Al_3Ti and TiB_2 at aluminium melting temperature is -4.31%. The misfit between Al and Al_3Ti is 0.085%. Although Al_3Ti is very coherent with aluminium, the misfit between TiB_2 and Al_3Ti is still quite large. This raises the question of how Al_3Ti is able to stay on TiB_2 despite their large misfit. This is the critical question for the following investigation.

Since there is no interatomic potential for boron available at present, the boron atoms were ignored. It is reasonable to take into account only the first nearest neighbors for the hexagonal TiB_2 structure since the first nearest neighbors have a dominant effect on hexagonal materials properties, not like the bcc structure where the second nearest neighbors are also important [25]. In addition, it has been suggested by DFT that TiB_2 has a Ti-terminated surface [26]. As a result, a single layer of titanium atoms with TiB_2 lattice spacing are placed at the bottom to represent TiB_2 substrate. The initial structure for MD is displayed in figure 1. The interfacial layer of Al_3Ti is taken to be epitaxial to the TiB_2 layer. The dimensions of TiB_2 and Al_3Ti are $34d_{[11\bar{2}]} \times 34d_{[\bar{1}10]} \times 1d_{[111]}$. In order to have a correct lattice spacing for aluminium, the dimensions of aluminium are $36d_{[11\bar{2}]} \times 36d_{[\bar{1}10]} \times 15d_{[111]}$. A vacuum of 30Å is added on the top along the [111] direction to eliminate the surface-surface interaction. Finally a very large-scale simulation cell was constructed.

For the MD process, NVT ensemble was employed and 1 femtosecond was taken for the timestep. Berendsen thermostat [27] was used for temperature control with a relaxation time of 0.1ps. First the melting temperature for aluminium will be examined. It is known that superheating will occur [28] if an infinite bulk aluminium sample is heated due to periodic condition. Hence, the coexistence method [29, 30] was employed to detect the melting temperature of aluminium. A melt of the above structure was prepared at 1200K and a hot
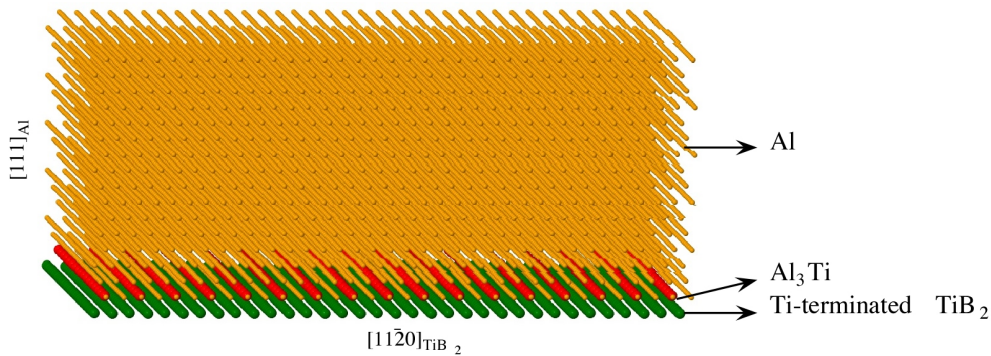
Figure 1. The initial structure used in MD simulations. The substrate Ti atoms within TiB$_2$ are colored green. The Ti atoms within Al$_3$Ti are colored red. The Al atoms are colored yellow.

solid was obtained at 800K. These two components were then combined together to generate a semisolid structure. Subsequently this semisolid structure was equilibrated between 800K and 900K. It can be found that the solid and liquid parts can exist at 850K, whereas the whole structure melts at 860K. Considering the statistical error bar within MD, the aluminium liquidus will be 855 ± 5 K. It is known that superheating can also occur for surface melting [28]. For example, the aluminium (111) surface melting has been detected to occur at 100K above its liquidus [31]. Therefore, the coexistence method was also employed here to construct the initial structure for investigations above the aluminium liquidus.

3. Results and analysis
The system was continuously heated and then equilibrated from 860K to 980K at intervals of 20K. During the simulation, the bottom titanium layer is fixed. We used a long time scale of 1000000 steps for each temperature. A structure at 860K was taken as an example shown in figure 2.
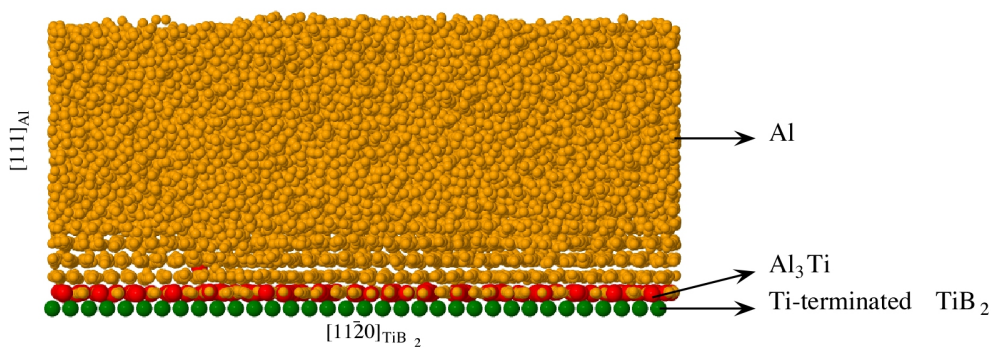

Figure 2. Equilibrated structure at 860K. The Ti atoms within TiB$_2$ are coloured green. The Ti atoms within Al$_3$Ti are colored red. The Al atoms are coloured yellow.

Figure 2 shows that the system displays a degree of layering adjacent to the TiB$_2$ surface. The structural layering can be characterised by a density profile $\rho(z)$ which quantifies the atomic distribution across the solid liquid interface [32]:

$$\rho(z) = \frac{N_z}{L_x L_y \Delta z},$$
(4)

where Δz is the slice of bin width parallel to the TiB$_2$ surface. L_x and L_y are the length of x and y directions, respectively. N_z is the number of atoms between $z - \Delta z/2$ and $z + \Delta z/2$. It is known that a proper bin should be selected in order to reduce the statistical error [32]. A small bin width could result in too few particles within a slice, whereas a large bin width will not show the real density profile of the system. We choose a reasonably fine bin width which was taken as the crystal d-spacing divided by 20. The density profiles at different temperatures are plotted in figure 3. Figure 3 shows that the atoms adjacent to the TiB$_2$ exhibit more order since
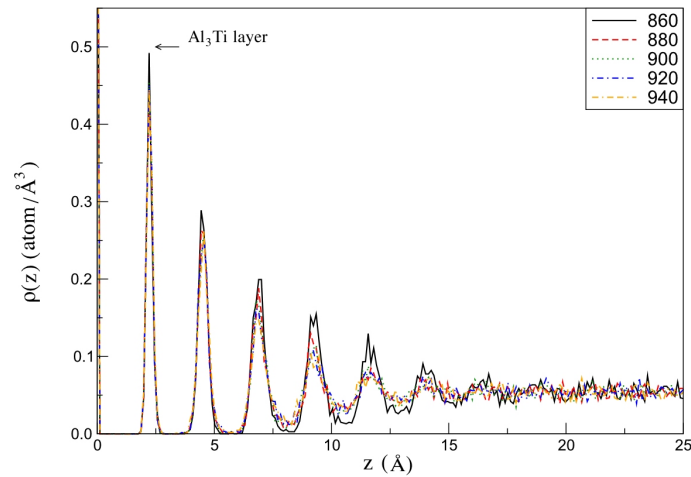

Figure 3. Density profile $\rho(z)$ of all atoms in the melt as a function of distance z. The corresponding temperatures are labelled in the legend.

they display narrower peaks with higher density. The sharp peak of Al$_3$Ti with high density shows that this layer is quite stable above aluminium liquidus. A common feature of the density profile is that they all decay gradually with respect to the distance z until a uniform density of the liquid phase is reached. The liquid phase density ρ_l was about 0.05 for our system.

To characterise the decay property at different temperatures, a quantitative measure of density profile was required. The decay of the density profile envelope can be effectively characterised by an exponential function [33, 32]:

$$\rho(z) = ae^{-\kappa z} + \rho_l, \qquad (5)$$

where a is a constant. The disorder parameter κ can be used to quantitatively describe the degree of disorder across the interface. First the density profile envelope in figure 3 is extracted, and then equation (5) is used to fit the density profile envelopes at different temperatures. The behaviour of κ is plotted in figure 4. Figure 4 shows that κ increases gradually with respect to temperature. Despite of this increase, it can still be seen from figure 3 that the Al$_3$Ti layer has the sharpest peak with the highest density which means this layer has a certain degree of order. Figure 5 displays the in-plane structure of the Al$_3$Ti layer. The triangular pattern in figure 5 implies that the layer of Al$_3$Ti undergoes interface reconstruction. The Al$_3$Ti are placed on TiB$_2$ according to different stacking sequences, denoted as red and blue area in figure 5, respectively. The triangles alternate with each other and have different orientations for their triangular patterns. These areas have very little strain. The transition area between these triangles is several atoms wide which is denoted as a green area in figure 5. This is a strain concentration area. By redistributing the strain, this interface reconstruction releases the large misfit strain between Al$_3$Ti and TiB$_2$. Although this mechanism for Al$_3$Ti/TiB$_2$ has not been verified experimentally, similar phenomena have been observed in other systems. For example, interface reconstruction
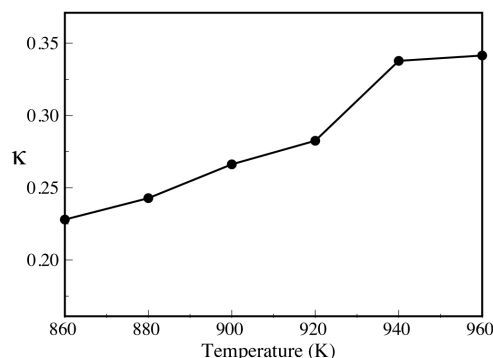
Figure 4. The disorder parameter κ with respect to temperature.

has been observed in Ag/Ru interface whose misfit is 7%.[1, 34]. The simulation on Ni/Al$_2$O$_3$ interface with a misfit of 9.3% also shows this type of interface reconstruction. Both Ag/Ru and Ni/Al$_2$O$_3$ display a triangular pattern for their interface reconstruction, similar to our results. This type of interface reconstruction is also termed a dislocation network [1, 34, 35].
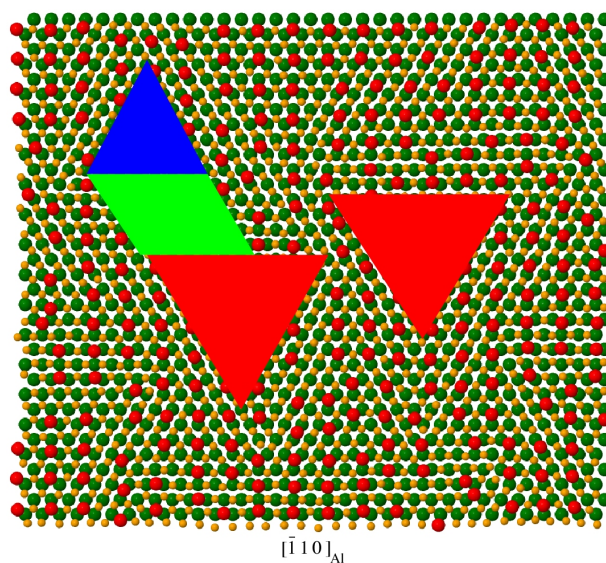

$[\bar{1}\,1\,0]_{Al}$

Figure 5. Ti-terminated TiB$_2$ surface and Al$_3$Ti layer at 860K. The Ti atoms within TiB$_2$ are colored green. The Ti atoms within Al$_3$Ti are colored red. The Al atoms are colored yellow. The different stacking sequences are shaded in red and blue, respectively. The transition area is shaded in green.

It differs from the regular misfit dislocation since the dislocation network cannot be analysed by drawing a Burgers circuit. This reconstructed Al$_3$Ti interface may stabilise this 2D Al$_3$Ti on the surface of TiB$_2$.

4. Conclusion
The interfacial Al$_3$Ti layer between TiB$_2$ and aluminium has been analysed by molecular dynamics. The results show that a 2D Al$_3$Ti layer may remain at the interface above aluminium liquidus. This interfacial Al$_3$Ti layer reconstructs itself by forming a triangular pattern in order to release the large misfit strain between TiB$_2$ and Al$_3$Ti. This triangular patter involves an

alternation of stacking sequences on TiB_2. The triangular parts are stainless area, but the transition region between the triangles is a strain concentration area. By localising the large misfit strain, the Al_3Ti layer is more stable on TiB_2. This observation is similar to that found in other systems which have been verified by experiments or simulations.

Due to the limitation of available interatomic potentials, boron atoms were ignored in these simulations. It is possible that the boron atoms increase the stability of the Al_3Ti layer. The simulations in this paper have indicated an interesting possible stabilisation mechanism for the Al_3Ti layer. We recognise this is the first step in our understanding of how how Al_3Ti can assist the nucleation of aluminium.

Acknowledgements

References
[1] Ling W L, de la Figuera J, Bartelt N C, Hwang R Q, Schmid A K, Thayer G E and Hamilton J C 2004 *Phys. Rev. Lett.* **92** 116102
[2] Cibula A 1951 *J. Inst. Metals* **80** 1–16
[3] Mohanty P S and Gruzleski J E 1996 *Acta Mater.* **44** 3749–3760
[4] Easton M and StJohn D 1999 *Metall. Mater. Trans. A* **30** 1613–1623
[5] Murty B S, Kori S A and Chakraborty M 2002 *Int. Mater. Rev.* **47** 3–29
[6] Quested T E 2004 *Mater. Sci. Technol.* **20** 1357–1369
[7] Quested T E 2004 *Solidification of Inoculated Aluminium Alloys* Ph.D. thesis University of Cambridge
[8] Wang J, Horsfield A, Lee P D and Brommer P 2010 *Phys. Rev. B* **82** 144203
[9] Schumacher P and Greer A L 1996 *Proceedings of the 1996 125th TMS Annual Meeting* (Anaheim, CA, USA) pp 745–753
[10] Hohenberg P and Kohn W 1964 *Phys. Rev.* **136** B864
[11] Kohn W and Sham L J 1965 *Phys. Rev.* **140** A1133
[12] Frenkel D and Smit B 2002 *Understanding molecular simulation: from algorithms to applications* 2nd ed (San Diego; London: Academic)
[13] Han Y, Dai Y, Shu D, Wang J and Sun B 2006 *Appl. Phys. Lett.* **89** 144107
[14] Wang J, Horsfield A, Schwingenschlögl U and Lee P D 2010 *Phys. Rev. B* **82** 184203
[15] Miao Y, Johnson J E and Ortoleva P J 2010 *J. Phys. Chem. B* **114** 11181–11195
[16] Smith W and Forester T R 1996 *J. Mol. Graphics* **14** 136–141
[17] Allen M P and Tildesley D J 1987 *Computer simulation of liquids* (Oxford: Clarendon Press)
[18] Finnis M W and Sinclair J E 1984 *Phil. Mag. A* **50** 45–55.
[19] Zope R R and Mishin Y 2003 *Phys. Rev. B* **68** 024102
[20] Mitra I and Telle R 1997 *J. Solid State Chem.* **133** 25–30
[21] Johnsson M and Eriksson L 1998 *Z. Metallkd.* **89** 478
[22] Norby P and Christensen A N 1986 *Acta Chem. Scand. A* **40** 157–159
[23] Smialek J L, Gedwill M A and Brindley P K 1990 *Scr. Metall. Mater.* **24** 1291–1296
[24] Kittel C 2005 *Introduction to solid state physics* 8th ed (New York: Wiley)
[25] Pettifor D G 1995 *Bonding and Structure of Molecules and Solids* (Oxford: Oxford University Press)
[26] Yanfeng H and et al 2006 *J. Phys.: Condens. Matter* **18** 4197
[27] Berendsen H J C, Postma J P M, Gunsteren W F v, DiNola A and Haak J R 1984 *J. Chem. Phys.* **81** 3684–3690
[28] Belonoshko A B, Skorodumova N V, Rosengren A and Johansson B 2006 *Phys. Rev. B* **73** 012201
[29] Morris J R, Wang C Z, Ho K M and Chan C T 1994 *Phys. Rev. B* **49** 3109
[30] Morris J R and Song X 2002 *J. Chem. Phys.* **116** 9352–9358
[31] Jin Z H and Lu K 1998 *Philos. Mag. Lett.* **78** 29 – 35
[32] Hashibon A, Adler J, Finnis M W and Kaplan W D 2002 *Comput. Mater. Sci.* **24** 443–452
[33] Tarazona P and Vicente L 1985 *Mol. Phys.* **56** 557 – 572
[34] Ling W L, Hamilton J C, Thürmer K, Thayer G E, de la Figuera J, Hwang R Q, Carter C B, Bartelt N C and McCarty K F 2006 *Surf. Sci.* **600** 1735–1757
[35] Long Y and Chen N X 2008 *J. Phys.: Condens. Matter* **20** 135005